



Trends of metals enrichment in deposited particulate matter at semi-arid area of Iran

Reza Fouladi Fard¹ · Kazem Naddafi^{2,3} · Mohammad Sadegh Hassanvand² · Mohammad Khazaei⁴ · Farah Rahmani⁵

Received: 6 November 2017 / Accepted: 13 April 2018 / Published online: 30 April 2018
© Springer-Verlag GmbH Germany, part of Springer Nature 2018

Abstract

The presence and enrichment of heavy metals in dust depositions have been recognized as an emerging environmental health issues in the urban and industrial areas. In this study, the deposition of some metals was found in Qom, a city located in a semi-desert area in Iran that is surrounded by industrial areas. Dust deposition samples were collected using five sampling stations during a year. Dust samples were digested applying acidic condition and then, the metal content was analyzed using inductively coupled plasma technology (ICP-OES). Comparative results showed the following order, from the maximum to the minimum concentration (mg/kg dust) of elements: Ca > Al > Fe > Mg > Ti > Si > K > B > Sr > Mn > P > Ba > Cr > Zn > Ni > Sn > Pb > V > Na > Cu > Co > U > Li > Ce > Ag. The differences among the average concentrations of metals in the five stations were not significant (p value > 0.05). The average concentration of some metals increased significantly during cold seasons. In this study, the cluster analysis (CA) and principal component analysis (PCA) were applied, and relationships among some elements in different clusters were found. In addition, the geo-accumulation and enrichment analysis revealed that the following metals had been enriched more than the average values: boron, silver, tin, uranium, lead, zinc, cobalt, chromium, lithium, nickel, strontium, and copper. The presence of thermal power plant, pesticide manufacturing plants, publishing centers, traffic jam, and some industrial areas around the city has resulted in the enrichment of some metals (particularly in cold seasons with atmospheric stable conditions) in dust deposition.

Keywords Dust deposition · Metals · Correlation analysis · Enrichment factors · Source assessment · Seasonal variation

Introduction

The atmospheric emission of pollutants has direct and indirect impacts on the environment and humans (Butean et al. 2014). The emissions of particle matters (PMs) in the atmosphere result from natural and anthropogenic sources (Rout et al. 2015). The atmospheric PMs are usually divided to suspended and settleable particles (Momani et al. 2000). Settleable particles or dustfalls are those particles that have excessive settling

velocity and short retention time in the atmosphere (Sipos et al. 2012). The settling velocity can be a function of the size and density of PMs. The PMs having aerodynamic diameter more than 10 μm are commonly known as “settleable particles” (Khuzestani and Souri 2013; Momani et al. 2000). PMs are also associated with cancer (class 1 carcinogenic according to the IARC) and cardiovascular mortality (Brunekreef and Holgate 2002). Dustfall is a hazardous and complex pollutant that has adverse effects on the human

Responsible editor: Responsible editor: Gerhard Lammel

✉ Kazem Naddafi
forhealthstudent@yahoo.com

¹ Research Center for Environmental Pollutants, Qom University of Medical Sciences, Qom, Iran

² Center for Air Pollution Research (CAPR), Institute for Environmental Research (IER), Tehran University of Medical Sciences, Tehran, Iran

³ Department of Environmental Health Engineering, School of Public Health, Tehran University of Medical Sciences, Tehran, Iran

⁴ Department of Environmental Health Engineering, School of Public Health and Research Center for Health Sciences, Hamadan University of Medical Sciences, Hamadan, Iran

⁵ Geological Survey of Iran, Medical Geology Department, Tehran, Iran

health (such as pneumonia, tonsillitis, allergy, and asthma), plants, and the environment (Cheng et al. 2008; Choi et al. 2008; Chung et al. 2003; De Longueville et al. 2010; Feng et al. 2012; Hamaiedh and El-Hasan 2011; Joshi et al. 2009; Qiao et al. 2013). The presence of heavy metals in dust deposition due to its toxicity has harmful effects on health (Kurt-Karakus 2012). The source of metals can be natural (such as volcanic activities, forest fires, and soil erosion) or anthropogenic such as industrial emissions, transportation, domestic usage of fuels, metal smelting, alloy refineries, cement manufacturing plant, municipal incinerator, and the construction emission activity (Boonyatumanond et al. 2007; Feng et al. 2012; Han et al. 2008; Harrad et al. 2009; Kvietskus et al. 2011; Lee et al. 2013; Sipos et al. 2012; Thakur et al. 2004; Wang et al. 2014; Yongming et al. 2006). Industrialization, urbanization, and motorization are the main causes of heavy metal depositions in the urban environments (Chen et al. 2014). Pollution associated with heavy metals in dust deposition is a serious problem due to its toxicity, carcinogenicity, non-biodegradable characteristics, and ability to accumulate the biota (Chen et al. 2014; Ghrefat et al. 2011; Khuzestani and Souri 2013; Melaku et al. 2008; Qiao et al. 2013). These depositions have significant effects on the terrestrial and aquatic ecosystems, as well as on biogeochemical cycles (Rashki et al. 2013; Soriano et al. 2012). The heavy metals in dust deposition can be absorbed by and accumulated into the internal organs and fatty tissues via direct inhalation, ingestion (e.g., from eating the plants that accumulate these metals), and dermal contact (Lu et al. 2009; Sharma and Agrawal 2005; Zheng et al. 2010). It may cause noxious effects on human health (such as central nervous system effects) and promote other diseases acting as cofactors (Dockery and Pope 1996; Nriagu 1988). The important indexes applied to identify the sources and the magnitude of metals in dust deposition are geo-accumulation index (I_{geo}), integrated pollution index (IPI), and enrichment factor (EF) (Ghrefat et al. 2011; Wei and Yang 2010). These indexes compare the current concentrations of metals with pre-industrial amounts and are applied to demonstrate the metals presence in various environments (Khuzestani and Souri 2013; Wei and Yang 2010). Metal depositions come from wet (rainfall) or dry precipitations and are collected during the sampling period into the collector located in an atmospheric environment. The passive sampling method used for dust and metal deposition in ambient environment provides valuable information regarding the influence of metals on the surface environment (Marrugo-Negrete et al. 2014; Wong et al. 2003). Assessing the content of metals in the atmospheric deposition has been carried out in the some parts of the world. This shows that there is a relation between the presence of industrial region and traffic jam and metals enrichment in dust depositions (Kara et al. 2014; Lynam et al. 2014; Marrugo-Negrete et al. 2014; Shakour Ali et al. 2011). To the authors' knowledge, there has been

no reliable study investigating the metal deposition in the urban environments located beside the central deserts of Iran (Kavir-e-Markazi), an area with a semi-arid climate and important ecological environments in the west part of Asia. Therefore, this study aimed to investigate metal deposition and enrichment in metropolitan city of Qom, located in the western bordering Kavir-e-Markazi that suffers from dust problems.

Materials and methods

Study area and sampling site

Qom is the capital city of Qom province and located at 34° 44' 37" N, to 55° 33' 27" E. It is a mega city with the population of approximately one million. The average elevation of the city is 950 m above the sea level. The annual average temperature and precipitation are 18.1 °C and 161 mm, respectively. Qom is an arid and semi-arid city in the central part of Iran on the banks of the Qom river in the vicinity of a desert (Kavir-e-Markazi) with low annual rainfall (Azarakhshi et al. 2012; Fouladi Fard et al. 2016; Isalou et al. 2014; Khadivi-Khub et al. 2015; Khazaei et al. 2013).

According to the American Society for Testing and Materials (ASTM) (D 1739) method for the collection of settleable particulate matter (Standard-ASTM 2004), five dust deposition sampling sites were selected in Qom, one of which was located in the center of the city and the rest belong to four divided municipal organization districts. Figure 1 illustrates the locations of sampling sites and wind rose of Qom in the sampling time period.

Sample collection

According to the ASTM guideline (D 1739), each sampling apparatus comprised of an open-topped plastic cylinder (dust container) supported by a stainless steel windshield and was mounted on a 2-m-high leg. Sampling apparatus were made and placed in appropriate sampling sites (no. 1 to no. 5, as can be observed in Fig. 1), which were located in open areas, free of natural obstacle (tree, hill, ...) or man-made structure (building, stack, ...), and higher than 1 m within a 20-m radius of the container stand. They were all continuously in-service for 1 year, from August 2012 to August 2013. After the end of each month (± 1 day), all five containers were removed simultaneously from sampling apparatus and replaced with five clean containers. The removed containers, comprising dustfall samples deposited (both of wet and dry depositions) during 1 month, were tightly closed and then transferred to the laboratory for further analysis. Collected dustfall samples were washed up with ultra-pure water, vacuum filtered via a Wattman white filter paper, and dried at 103–105 °C. Dried

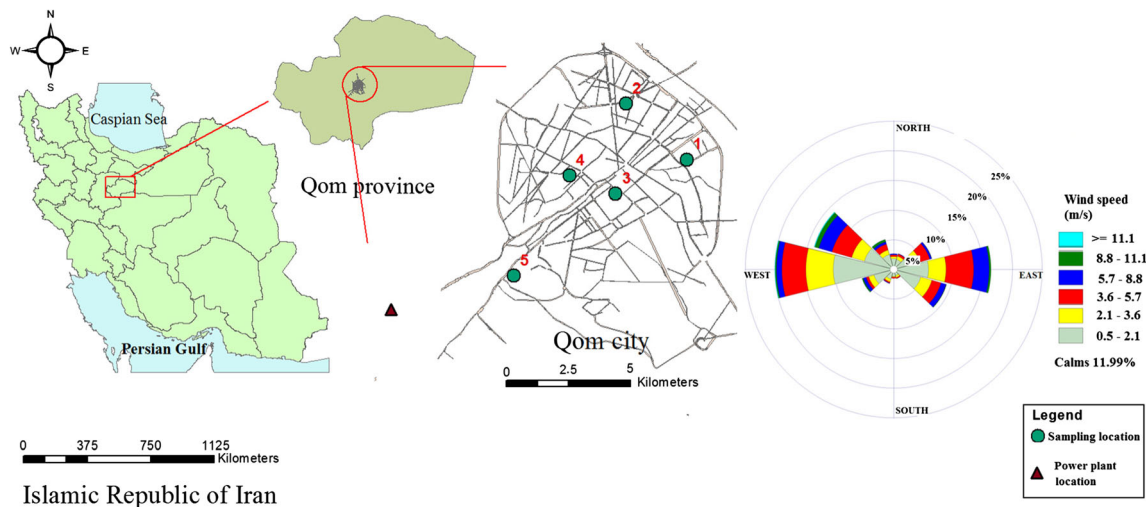


Fig. 1 Sampling site locations and wind rose of the study area (no. 1: Rural Water and Wastewater Company (RWWC), no. 2: Shadid Beheshti Hospital (SBH), no. 3: School of Public Health, Qom University of

Medical Sciences (SPH), no. 4: Education Office (EO), and no. 5: Municipal Water and Wastewater Company (MWWC))

samples (nonsoluble dust on the filter and soluble fraction in the crucible) were then stored in polyethylene bags for further metal analysis. After the sampling process was over, the containers were cleaned with distilled water and 1% nitric acid solution (Soriano et al. 2012).

Chemical analysis

Each dust sample was digested with an acid mixture on a hot plate (Hsu et al. 2008). Dusts and filters (both of them) were immersed in Teflon beakers with an acid mixture (5 ml HF, 10 ml HNO₃, and 0.5 ml HClO₄). The solution was vacuum dried under the temperature around 200 °C. The residue was re-dissolved in concentrated HNO₃ and HCl mixtures and then heated to complete the digestion process. The remaining filters were removed with tweezers and rinsed with ultra-pure water. One clean filter (in each series of digestion) was digested for correction of the amount of metals in the filter as a blank value. The resulting solution was filtered and diluted to the volume of 50 ml. Finally, the prepared solution was examined to find the concentration of various elements (Ag, Al, B, Ba, Ca, Ce, Co, Cr, Cu, Fe, K, Li, Mg, Mn, Na, Ni, P, Pb, Si, Sn, Sr, Ti, U, V, and Zn) by using inductively coupled plasma-optical emission spectrometer (ICP-OES) model VARIAN 735-ES. The limit of detection for metal analysis was 0.01 ppm. Standard aqueous samples containing metal mixture were prepared by dilution from the respective 1000 ppm standard solution (VHG, SM35A-XXX).

Assessment of the level of contamination

Contamination levels of metals in the settleable dust samples were evaluated by applying the geo-accumulation index (I_{geo}) and enrichment factor (EF). The I_{geo} was originally used for

bottom sediments and was firstly introduced by Müller (1969). The I_{geo} is also widely used for the assessment of heavy metal content in dusts (Chen et al. 2014; Feng et al. 2012; Khuzestani and Souri 2013; Lee et al. 2013; Wang et al. 2014; Wei and Yang 2010) and can be calculated by the following equation (Eq. 1):

$$I_{geo} = \log_2 \left(\frac{C_n}{1.5B_n} \right) \tag{1}$$

where C_n represents the concentration of the measured element “ n ” in the deposited dust and B_n is the geochemical background value of the element “ n ” (Wang et al. 2014). In the current study, the global average of elemental concentrations for continental crust, provided by Taylor (1964), has been used as the background reference values for the assessment of contamination levels. The constant value of 1.5 is the correction factor for possible variations of background data from lithological variability (Khuzestani and Souri 2013; Lee et al. 2013). Table 1 presents seven classes of contamination levels according to the different I_{geo} values proposed by Müller (1969) (Feng et al. 2012; Khuzestani and Souri 2013).

Table 1 Classification of I_{geo} contamination levels

I_{geo} value	Class	Contamination Level
≤ 0	0	Untamminated
0–1	1	Untamminated to moderately contaminated
1–2	2	Moderately contaminated
2–3	3	Moderately to heavily contaminated
3–4	4	Heavily contaminated
4–5	5	Heavily to extremely contaminated
> 5	6	Extremely contaminated

In order to gain a further insight into the origins of heavy metals, the EF was also applied. The EF is based on the standardization of a measured metal against a reference one and can be calculated by the following equation (Eq. 2):

$$EF = \left[\frac{(C_{E,D}/C_{Al,D})}{\left(\frac{C_{E,C}}{C_{Al,C}}\right)} \right] \quad (2)$$

where $C_{E,D}$ and $C_{Al,D}$ are the elemental and aluminum concentrations in sample settleable dust, respectively. Likewise, $C_{E,C}$ and $C_{Al,C}$ are the elemental and aluminum concentrations in average crustal rock, respectively (Lue et al. 2010; Lynam et al. 2014; Mijić et al. 2010). Aluminum was considered as a reference element because of its low occurrence variability, like the other dust contamination assessments (Chen et al. 2014; Lue et al. 2010; Lynam et al. 2014; Mijić et al. 2010; Shakour Ali et al. 2011).

The values obtained from Eq. 2 show the elemental enrichment. Values less than 1 indicate “no enrichment.” Values in the range of 1–3, 3–5, 5–10, 10–25, and 25–50 indicate “minor enrichment,” “moderate enrichment,” “moderately severe enrichment,” “severe enrichment,” and “very severe enrichment,” respectively. Finally, values more than 50 indicate “extremely severe enrichment” (Khuzestani and Souri 2013).

Statistical analysis

The one-way analysis of variance (ANOVA) was applied to compare the amount of the elements deposited in sampling sites and different seasons, after adjusting the effect of extreme value and Ln transformation. The Tukey post hoc test was used when the ANOVA test was significant. The principal component analysis (PCA) and cluster analysis (CA) methods, which are usually applied in the environmental studies, were used as multivariate analysis (Kara et al. 2014; Qiao et al. 2013; Rout et al. 2015; Yongming et al. 2006). These methods are effective to recognize the source and elemental distribution of dust samples (Qiao et al. 2013). PCA was used to assign the wide range of concentrations obtained in the study. This analysis can be employed to identify patterns and examine the similarities and differences (Shin et al. 2010). The data and variables were normalized to a unit variance for analysis according to the same proportion. To obtain more obvious interpretations, varimax rotation with Kaiser normalization was used. For classifying the measured elements, a hierarchical CA was also applied. CA clusters the elements together based on their chemical similarity. In addition, CA is helpful for selecting similar groups and can be served as a supplementary for PCA (Yongming et al. 2006). Dendrogram diagram was used to show the assignment of elements to their

clusters. To standardize the concentration data in the CA, Ward’s method was used. Cluster analysis using Ward’s method was used to generate dendrogram for estimation of the number of likely clusters within the studied parameters (Haldar et al. 2008). Statistical analyses were performed with SPSS software (version 20.0).

Results and discussion

Dust elemental concentrations, station, and seasonal variation

The annual arithmetic mean concentrations, maximum, minimum, and standard deviation (SD) of metals in dust deposition are shown in Table 2. The annual average of metal concentrations in all sampling stations revealed the following decreasing order:

$$\begin{aligned} \text{Ca} > \text{Al} > \text{Fe} > \text{Mg} > \text{Ti} > \text{Si} > \text{K} > \text{B} > \text{Sr} > \text{Mn} > \text{P} \\ > \text{Ba} > \text{Cr} > \text{Zn} > \text{Ni} > \text{Sn} > \text{Pb} > \text{V} > \text{Na} > \text{Cu} \\ > \text{Co} > \text{U} > \text{Li} > \text{Ce} > \text{Ag}. \end{aligned}$$

Figure 2 shows the box plot of measured element concentration. As shown in Fig. 2, regarding the wide range of element concentrations (from 70.06×10^3 g/kg dust for Ca to 0.51 g/kg dust for Cr), the vertical axis of diagram is scaled logarithmically. Based on the results, the minimum, 25%, median, 75%, maximum, the outlier, and the extreme amounts of elements can be identified. The concentration of calcium, aluminum, and iron is obviously greater than the concentration in other elements. Similar findings were also obtained in some regions of India and Turkey regarding the highest contents of abovementioned elements in dust deposition (Kara et al. 2014; Rout et al. 2015). In addition to soil origin of iron and aluminum, these elements might originate from anthropogenic sources such as vehicles (Gunawardana et al. 2012; Mun’im Mohd Han et al. 2014).

As shown in Fig. 1, the sampling sites were RWWC (eastern north), SBH (north), SPH (center), EO (west), and MWWC (south), covering four geographical directions plus a center point. Figure 3a illustrates the annual arithmetic average concentration of different elements in dust depositions (mg/kg dust) reported by each sampling station. It was observed that there were no significant differences among the element concentration in different sites with the one-way ANOVA test. Furthermore, depending on the distance of sampling stations from pollution sources (industrial estates, urban traffic jam ...), significant differences among element concentrations in some surveys were reported. According to a study in Colombia, the existence of a mining area in the vicinity of

Table 2 Descriptive statistics of annual element concentration with crustal backgrounds (mg/kg)

Element	Arithmetic mean	Max	Min	SD	B_n^*	$\left(\frac{C_{E.C.}}{C_{ALC.}}\right)$
Ag	4.46E + 00	2.72E + 01	6.01E - 01	4.92E + 00	8.51E - 07	7.00E - 02
Al	2.83E + 04	6.25E + 04	1.03E + 04	1.04E + 04	1.00E + 00	8.23E + 04
B	1.21E + 03	6.67E + 03	2.77E + 00	1.47E + 03	1.22E - 04	1.00E + 01
Ba	1.89E + 02	3.98E + 02	4.61E + 01	8.89E + 01	5.16E - 03	4.25E + 02
Ca	4.30E + 04	7.01E + 04	5.47E + 03	1.49E + 04	5.04E - 01	4.15E + 04
Ce	2.40E + 01	5.65E + 01	2.32E + 00	1.14E + 01	7.29E - 04	6.00E + 01
Co	5.40E + 01	1.51E + 02	1.95E + 01	2.15E + 01	3.04E - 04	2.50E + 01
Cr	1.73E + 02	1.30E + 03	5.15E - 01	2.63E + 02	1.22E - 03	1.00E + 02
Cu	6.42E + 01	2.22E + 02	1.29E + 01	4.49E + 01	6.68E - 04	5.50E + 01
Fe	1.78E + 04	4.00E + 04	7.13E + 03	6.39E + 03	6.84E - 01	5.63E + 04
K	1.22E + 03	2.10E + 03	3.18E + 02	4.62E + 02	2.54E - 01	2.09E + 04
Li	3.03E + 01	5.73E + 01	1.31E + 01	9.88E + 00	2.43E - 04	2.00E + 01
Mg	6.43E + 03	1.56E + 04	1.54E + 03	2.78E + 03	2.83E - 01	2.33E + 04
Mn	3.88E + 02	9.07E + 02	1.18E + 02	1.50E + 02	1.15E - 02	9.50E + 02
Na	7.37E + 01	1.92E + 02	2.47E + 01	3.54E + 01	2.87E - 01	2.36E + 04
Ni	1.08E + 02	6.40E + 02	6.33E - 01	1.25E + 02	9.11E - 04	7.50E + 01
P	3.77E + 02	8.47E + 02	1.13E + 02	1.64E + 02	1.28E - 02	1.05E + 03
Pb	7.63E + 01	3.91E + 02	2.46E + 01	6.27E + 01	1.52E - 04	1.25E + 01
Si	1.56E + 03	1.00E + 04	2.52E + 01	2.21E + 03	3.42E + 00	2.82E + 05
Sn	8.88E + 01	5.88E + 02	1.46E + 00	1.16E + 02	2.43E - 05	2.00E + 00
Sr	4.99E + 02	7.40E + 02	7.99E + 01	1.71E + 02	4.56E - 03	3.75E + 02
Ti	1.58E + 03	3.14E + 03	4.63E + 02	6.07E + 02	6.93E - 02	5.70E + 03
U	4.12E + 01	1.02E + 02	2.09E + 01	1.57E + 01	3.28E - 05	2.70E + 00
V	7.51E + 01	1.45E + 02	2.72E + 01	2.55E + 01	1.64E - 03	1.35E + 02
Zn	1.67E + 02	4.86E + 02	2.67E + 01	1.11E + 02	8.51E - 04	7.00E + 01

* B_n , geochemical background (Taylor 1964)

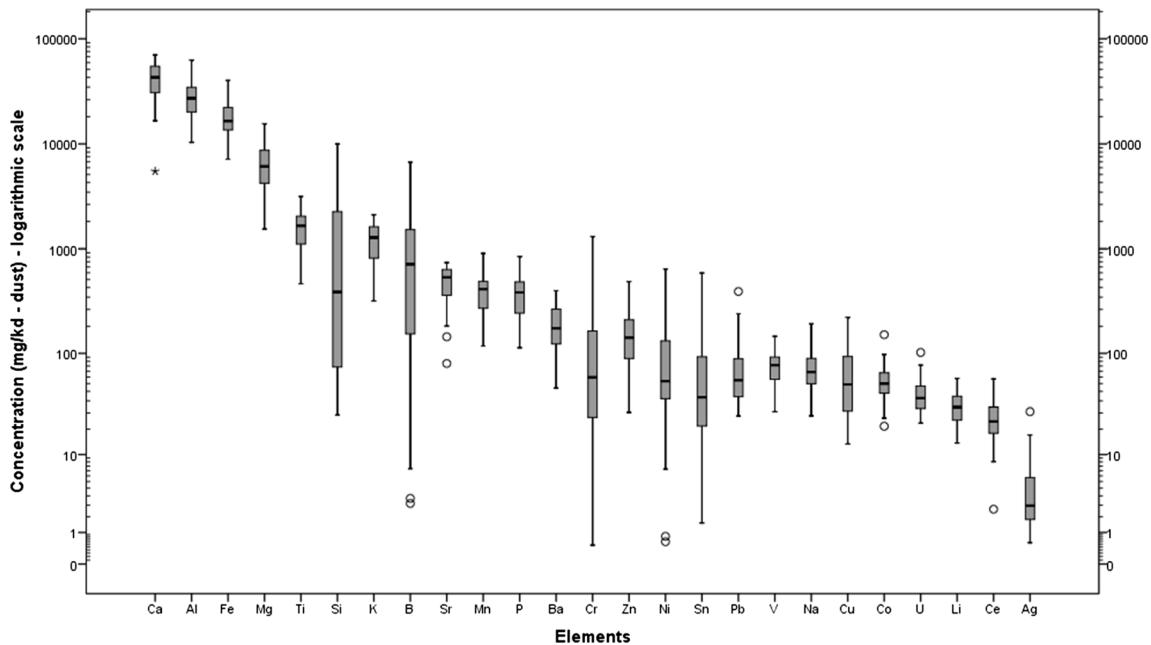


Fig. 2 Box plot with outlier (o) and extreme (*) values for dust deposition elements for all stations (in five sampling stations, based on monthly sampling in 1 year)

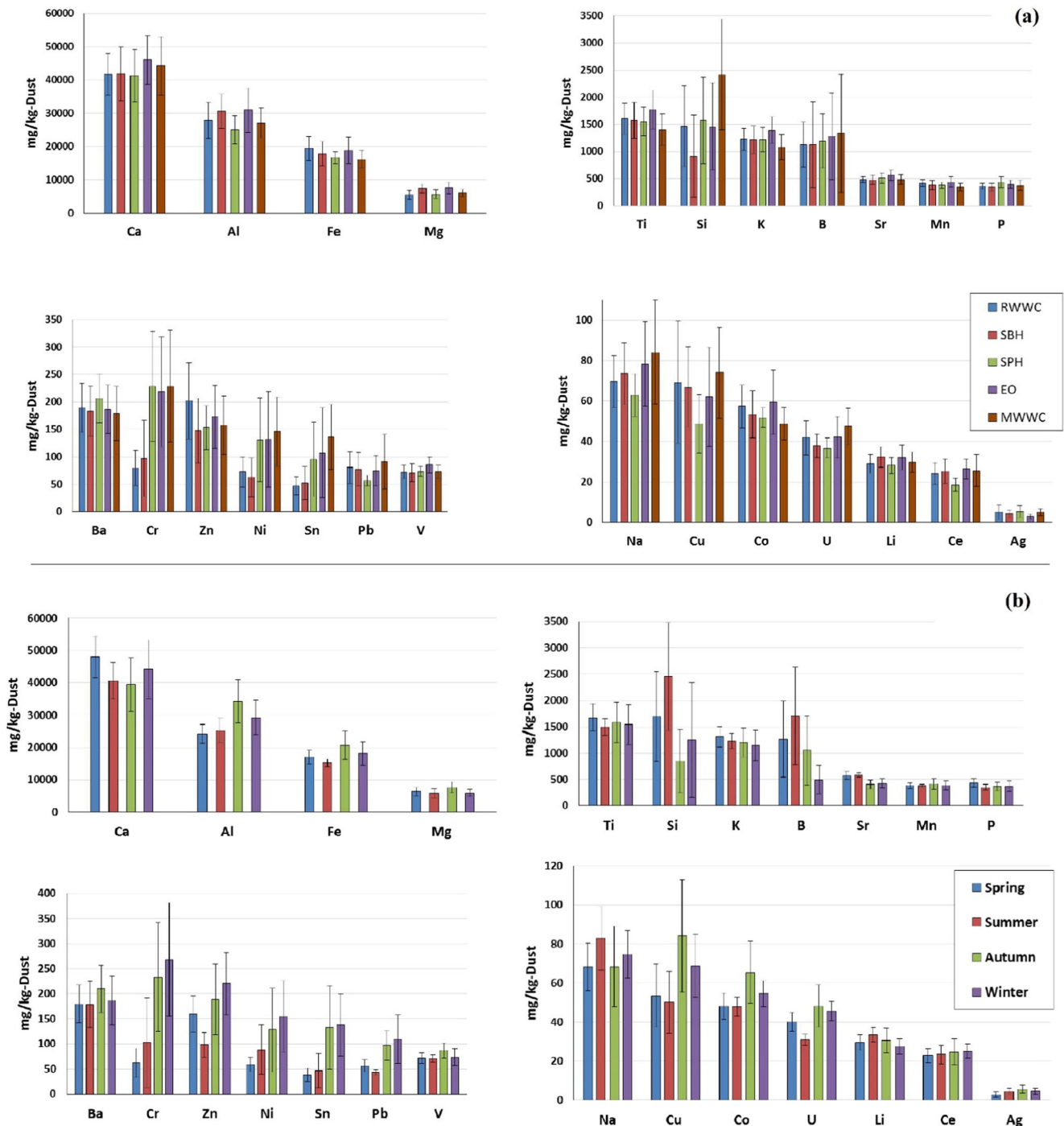


Fig. 3 Annual arithmetic mean of deposited elements in different sampling stations (a) and seasonal arithmetic mean of different deposited elements in all sampling stations (b)

the sampling site leads to significant differences among the heavy metal contents (Marrugo-Negrete et al. 2014).

Regarding all sampling sites, Fig. 3b shows the seasonal arithmetic average of various elements in dust deposition. One-way ANOVA test results showed that there were significant differences among concentrations of Al ($p = 0.03$), Cr ($p = 0.03$), Pb ($p = 0.001$), Sn ($p = 0.004$), U ($p = 0.01$), and Zn ($p = 0.016$) in different seasons. Except the Al that had

the greatest amount in autumn, the majority of other elements had the highest amount in the winter. The concentration of Al decreased as follows: autumn > winter > summer > spring; of U, Pb, and Zn: winter > autumn > spring > summer; and of Cr and Sn: winter > autumn > summer > spring. The concentration of Ni ($p = 0.101$), Cu ($p = 0.141$), and Co ($p = 0.083$) in the winter and autumn considerably increased in spring and summer, yet these differences were not statistically significant.

Additionally, the concentrations of Si ($p = 0.055$) and B ($p = 0.112$) in the spring and summer were more than those in the autumn and winter, but these differences were not statistically significant. Also, two-factor ANOVA showed that, in all metal concentrations, there were no significant interaction between station and season. In the cold seasons, the dust may originate from internal sources (i.e., traffic, internal, and surrounding industries) rather than from external sources (around deserts like Kavir-e- Markazi). This can be attributed to the more stable weather conditions in the cold seasons (according to the hourly meteorological data of Qom (IRIMO-Qom 2013), the 42% of hours in the autumn and winter belong to the stable E, F, and G pasquill classes compared with 37% in the spring and summer). This may cause a high concentration of mentioned metals in cold seasons. On the other hand, in the summer and spring (warm seasons), the contribution of external sources (natural source) probably increased and the amount of metals in the dust decreased. In other studies, the higher concentration of heavy metals in the winter and other seasons has also been reported (Bellis et al. 2005; Moja and Mnisi 2013; Pandey et al. 2008; Rout et al. 2015).

Correlation analysis between dust elements

The results of correlation among different concentration of elements using Pearson analysis are summarized in Table 3. As represented in this table, the elements are arranged in a pairwise matrix framework. So, the correlation between each metals by itself should be equal to 1. The numbers appeared on the left-bottom side of the table represent Pearson correlation coefficients, and the numbers shown on the right-top side of the table represent significant levels. As shown in Table 3, except for elements including Ni, Cr, Ag, and Sn, the significantly positive correlation of other elements was approximately obtained together, indicating their common source. Furthermore, a significantly positive relationship was found both among Sn, Ag, Cr, and Ni and between these elements and Pb and U, thus showing the probability of the existence of a common source (industrial and/or traffic) for all of them.

Multivariate analysis

Table 4 shows the output results from PCA. As shown in Table 4, data were classified in four components, and in each component, the PCA loadings > 0.45 represent the membership of elements in the same group. For example, in the first component, Ca, Ba, Co, Cu, Fe, K, Mn, P, Pb, Ti, U, V, and Zn can be categorized as a group. This group of elements may have soil or crust re-suspension origin.

The existence of a correlation among elements such as Mg, K, Fe, and Ca attributed to the source of earth crust was reported in the study by Rout et al. (2015). There were Al, Ce, Li, and Mg in the second component that can be derived from

natural sources. Ag, Cr, Ni, and Sn belonged to the third component that can be attributed to the anthropogenic sources. Elements such as B, Na, and Si, which belonged to the fourth component, can result from the industries and ambient salt deserts. Figure 4a shows a three-dimensional framework to illustrate the PCA loadings for different elements. The results of PCA for different elements in Jharia (India) dust deposition showed three components: natural, mining, and anthropogenic sources (Rout et al. 2015). The PCA applied for an industrial area dust deposition in Turkey showed that the measured elements were classified into five components, and soil, industry, residential, and traffic sources were finally suggested (Kara et al. 2014).

Also, the results of cluster analysis are displayed by a dendrogram in Fig. 4b. As a result, the measured elements in dust deposition are classified in seven clusters (separated by red rectangle). The length of lines in Fig. 4b indicates the strength of correlation among different elements, the short length of connecting lines to the elements, and the strong correlation between those elements. For example, in the top cluster of Fig. 4b, Mn and V have been joined together at a relatively high level of correlation than those of Pb and U. Thus, it can be concluded that those clusters that have shorter lines might be emitted from common sources (Yongming et al. 2006).

Elemental enrichment and geo-accumulation in dust deposition

The average background concentration (B_n) of elements and the ratio of average background concentration of each element per background concentration of aluminum ($C_{E,C} / C_{Al,C}$) have been presented in Table 2. The I_{geo} value, I_{geo} class, and enrichment factor of each element were calculated according to Eqs. 1 and 2 for all four seasons (as well as for annual average concentration) as shown in Table 5 and for various sampling stations as outlined in Table 6. According to Table 5, B (EF 352.26—class 6 I_{geo}), Ag (EF 185.46—class 6 I_{geo}), Sn (EF 129.26—class 5 I_{geo}), U (EF 44.42—class 4 I_{geo}), and Pb (EF 17.77—class 3 I_{geo}) have the maximum enrichment in dust deposition. Moreover, the metals such as Co (EF = 6.29), Cr (EF = 5.04), and Zn (EF = 6.93) in the class 1 of I_{geo} had moderately severe enrichments. The metals such as Ni (EF = 4.2), lithium (EF = 4.4), copper (EF = 3.4), and strontium (EF = 3.87) had also moderate enrichments.

Although boron (B) is an essential nutrient for plants, its high accumulation can be toxic for organisms (Çöl and Çöl 2003). The amounts of enriched B in this region can be due to the existence of insecticide and pesticide companies (Çöl and Çöl 2003; Woods 1994) surrounding the city (there are two nationally famous insecticide companies in the region) and the high rate of pesticide usage in the farmlands around the city. Besides, other sources such as fossil fuel combustion, ceramics, fiberglass, and detergent industrials have also been

Table 3 Pearson's correlation matrix for the element concentrations

	Ag	Al	B	Ba	Ca	Ce	Co	Cr	Cu	Fe	K	Li	Mg													
Ag	1																									
Al	0.11	1																								
B	-0.08	0.17	1																							
Ba	0.23	0.60**	0.58**	1																						
Ca	0.12	0.48**	0.42**	0.74**	1																					
Ce	0.20	0.64**	0.52**	0.70**	0.66**	1																				
Co	0.28*	0.76**	0.34**	0.78**	0.59**	0.66**	1																			
Cr	0.49**	0.13	-0.10	0.04	-0.12	0.06	0.28*	1																		
Cu	0.20	0.56**	0.45**	0.73**	0.56**	0.55**	0.70**	0.08	1																	
Fe	0.24	0.76**	0.41**	0.83**	0.71**	0.69**	0.96**	0.18	0.75**	1																
K	-0.05	0.60**	0.68**	0.80**	0.82**	0.70**	0.69**	-0.16	0.60**	0.78**	1															
Li	0.10	0.70**	0.59**	0.66**	0.72**	0.68**	0.68**	-0.04	0.62**	0.73**	0.82**	1														
Mg	0.11	0.83**	0.25	0.55**	0.57**	0.58**	0.65**	0.00	0.58**	0.68**	0.59**	0.73**	1													
Mn	0.17	0.66**	0.63**	0.84**	0.82**	0.77**	0.85**	0.04	0.67**	0.89**	0.92**	0.84**	0.84**	1												
Na	0.11	0.55**	0.68**	0.72**	0.74**	0.73**	0.68**	0.03	0.76**	0.73**	0.79**	0.84**	0.57**	0.57**	1											
Ni	0.38**	-0.08	-0.17	0.02	0.08	0.04	0.15	0.68**	0.18	0.13	-0.07	-0.08	0.01	0.01	0.01	1										
P	0.13	0.56**	0.64**	0.83**	0.81**	0.71**	0.72**	-0.07	0.68**	0.80**	0.92**	0.78**	0.57**	0.57**	0.57**	0.57**	1									
Pb	0.31*	0.66**	0.23	0.66**	0.52**	0.50**	0.80**	0.31*	0.78**	0.82**	0.51**	0.50**	0.56**	0.56**	0.56**	0.56**	0.56**	1								
Si	0.00	0.28*	0.90**	0.67**	0.59**	0.60**	0.58**	0.02	0.54**	0.58**	0.72**	0.67**	0.32*	0.32*	0.32*	0.32*	0.32*	0.32*	1							
Sn	0.22	0.20	-0.23	-0.02	-0.12	-0.01	0.26	0.89**	0.22	0.18	-0.22	-0.08	0.06	0.06	0.06	0.06	0.06	0.06	0.06	1						
Sr	-0.02	0.43**	0.63**	0.69**	0.86**	0.64**	0.54**	-0.17	0.45**	0.63**	0.87**	0.81**	0.47**	0.47**	0.47**	0.47**	0.47**	0.47**	0.47**	0.47**	1					
Ti	0.02	0.65**	0.66**	0.82**	0.81**	0.72**	0.75**	-0.06	0.65**	0.83**	0.98**	0.85**	0.61**	0.61**	0.61**	0.61**	0.61**	0.61**	0.61**	0.61**	0.61**	1				
U	0.29*	0.63**	0.15	0.61**	0.68**	0.51**	0.70**	0.22	0.74**	0.77**	0.56**	0.56**	0.62**	0.62**	0.62**	0.62**	0.62**	0.62**	0.62**	0.62**	0.62**	0.62**	1			
V	0.08	0.67**	0.52**	0.79**	0.71**	0.69**	0.86**	0.19	0.64**	0.87**	0.91**	0.79**	0.60**	0.60**	0.60**	0.60**	0.60**	0.60**	0.60**	0.60**	0.60**	0.60**	0.60**	1		
Zn	0.26	0.47**	0.36*	0.71**	0.65**	0.50**	0.67**	0.14	0.75**	0.74**	0.66**	0.51**	0.47**	0.47**	0.47**	0.47**	0.47**	0.47**	0.47**	0.47**	0.47**	0.47**	0.47**	0.47**	0.47**	1

	Mn	Na	Ni	P	Pb	Si	Sr	Sn	Ti	U	V	Zn
Ag	0.24	0.44	0.01	0.36	0.03	0.99	0.89	0.12	0.90	0.04	0.58	0.06
Al	0.00	0.00	0.58	0.00	0.00	0.03	0.00	0.15	0.00	0.00	0.00	0.00
B	0.00	0.00	0.28	0.00	0.13	0.00	0.00	0.13	0.00	0.32	0.00	0.01
Ba	0.00	0.00	0.89	0.00	0.00	0.00	0.00	0.88	0.00	0.00	0.00	0.00
Ca	0.00	0.00	0.56	0.00	0.00	0.00	0.00	0.38	0.00	0.00	0.00	0.00
Ce	0.00	0.00	0.75	0.00	0.00	0.00	0.00	0.97	0.00	0.00	0.00	0.00
Co	0.00	0.00	0.27	0.00	0.00	0.00	0.00	0.05	0.00	0.00	0.00	0.00
Cr	0.79	0.83	0.00	0.59	0.02	0.91	0.23	0.00	0.65	0.11	0.18	0.30
Cu	0.00	0.00	0.18	0.00	0.00	0.00	0.00	0.10	0.00	0.00	0.00	0.00
Fe	0.00	0.00	0.34	0.00	0.00	0.00	0.00	0.18	0.00	0.00	0.00	0.00
K	0.00	0.00	0.59	0.00	0.00	0.00	0.00	0.10	0.00	0.00	0.00	0.00
Li	0.00	0.00	0.54	0.00	0.00	0.00	0.00	0.56	0.00	0.00	0.00	0.00
Mg	0.00	0.00	0.94	0.00	0.00	0.01	0.00	0.68	0.00	0.00	0.00	0.00

Table 3 (continued)

	Mn	Na	Ni	P	Pb	Si	Sn	Sr	Ti	U	V	Zn
Mn	1	0.00	0.80	0.00	0.00	0.00	0.85	0.00	0.00	0.00	0.00	0.00
Na	0.81**	1	0.65	0.00	0.00	0.00	0.71	0.00	0.00	0.00	0.00	0.00
Ni	0.03	0.06	1	0.69	0.07	0.74	0.00	0.39	0.96	0.02	0.54	0.02
P	0.9**	0.79**	0.05	1	0.00	0.00	0.40	0.00	0.00	0.00	0.00	0.00
Pb	0.65**	0.58**	0.24	0.58**	1	0.01	0.00	0.02	0.00	0.00	0.00	0.00
Si	0.74**	0.79**	-0.05	0.75**	0.35**	1	0.32	0.00	0.00	0.01	0.00	0.00
Sn	-0.03	0.05	0.66**	-0.12	0.43**	-0.14	1	0.05	0.46	0.00	0.32	0.08
Sr	0.84**	0.78**	-0.12	0.84**	0.31*	0.72**	-0.27	1	0.00	0.00	0.00	0.00
Ti	0.94**	0.80**	-0.01	0.94**	0.58**	0.74**	-0.10	0.85**	1	0.00	0.00	0.00
U	0.66**	0.61**	0.30*	0.65**	0.82**	0.34**	0.38**	0.44**	0.62**	1	0.00	0.00
V	0.97**	0.71**	0.09	0.88**	0.68**	0.70**	0.14	0.75**	0.94**	0.62**	1	0.00
Zn	0.71**	0.64**	0.31*	0.72**	0.74**	0.51**	0.24	0.47**	0.73**	0.73**	0.66**	1

The left lower part is correlation coefficient; the right upper part is significant level

* $p < 0.05$ (2-tailed)

** $p < 0.01$ (2-tailed)

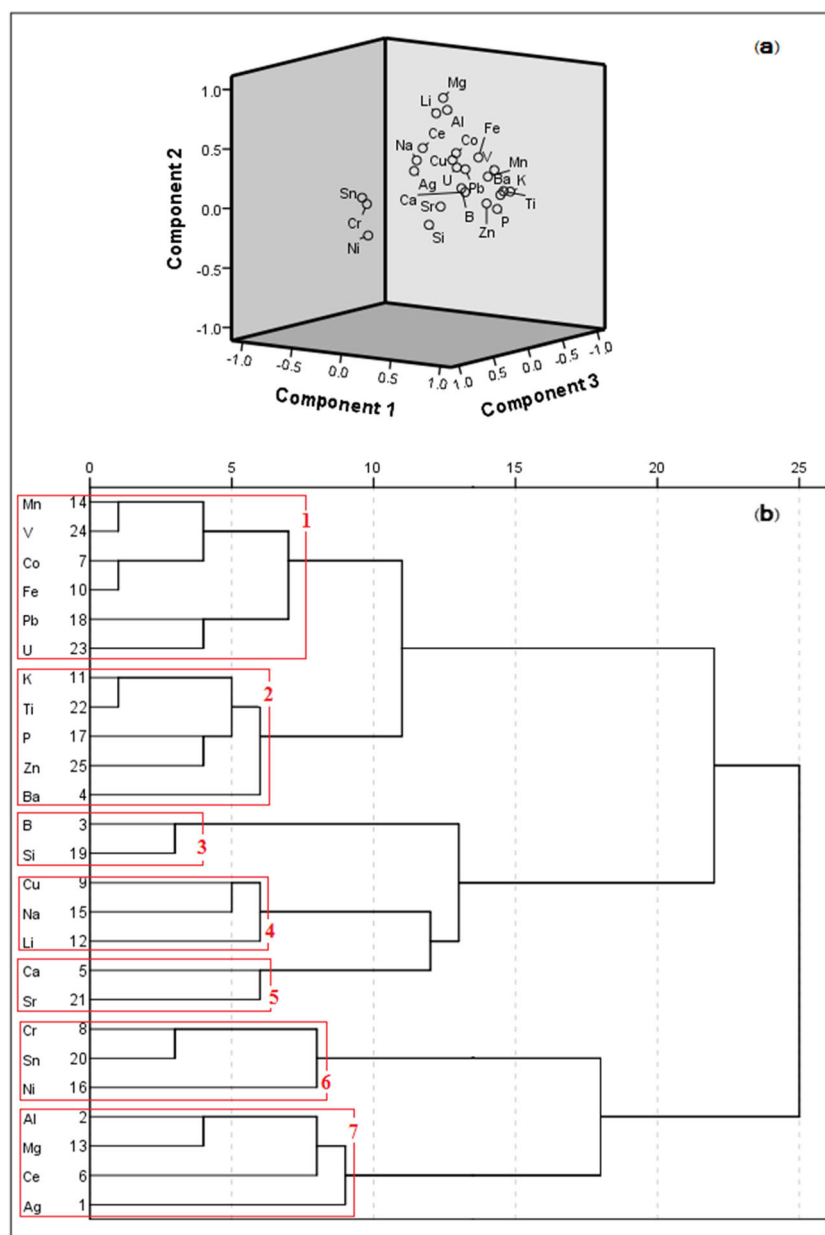
Table 4 Rotated component matrix (Extraction method: principal component analysis; rotation method: varimax with Kaiser normalization. Rotation converged in 7 iterations. Factor loadings > 0.45 are shown in italics) for data of dust deposition samples

Element	Components			
	1	2	3	4
Ag	0.293	0.365	<i>0.477</i>	-0.237
Al	0.397	<i>0.843</i>	0.149	-0.154
B	0.367	0.144	-0.101	<i>0.845</i>
Ba	<i>0.830</i>	0.149	-0.001	0.246
Ca	<i>0.483</i>	0.140	0.012	-0.072
Ce	0.348	<i>0.558</i>	0.433	0.121
Co	<i>0.664</i>	<i>0.542</i>	0.402	0.102
Cr	0.071	0.118	<i>0.843</i>	0.223
Cu	<i>0.522</i>	0.448	0.251	0.311
Fe	<i>0.801</i>	<i>0.502</i>	0.274	0.030
K	<i>0.824</i>	0.155	-0.153	0.200
Li	0.210	<i>0.780</i>	0.040	0.314
Mg	0.205	<i>0.893</i>	-0.067	-0.046
Mn	<i>0.839</i>	0.332	0.192	0.168
Na	0.227	0.429	0.345	<i>0.523</i>
Ni	0.066	-0.152	<i>0.817</i>	-0.162
P	<i>0.815</i>	0.032	0.022	0.078
Pb	<i>0.734</i>	0.409	0.367	0.028
Si	0.241	-0.135	0.188	<i>0.889</i>
Sn	0.080	0.184	<i>0.925</i>	0.171
Sr	0.136	-0.038	-0.129	0.283
Ti	<i>0.892</i>	0.193	0.042	0.241
U	<i>0.628</i>	0.409	0.340	-0.075
V	<i>0.840</i>	0.374	0.098	0.237
Zn	<i>0.823</i>	0.104	0.187	0.147

reported to be related to B (Parks and Edwards 2005; Yazbeck et al. 2005). The great amount of silver, considerably in downtown areas, can be a result of the existence of numerous publishing centers in the area (Purcell and Peters 1998). The city of Qom has the largest number of small publishing companies and large publishing industries in Iran.

With regard to the seasons, it is obvious that the enrichment of Cr, Cu, Ni, Pb, Sn, and Zn in the winter and autumn is higher than it is in the spring and summer. Weather condition in the autumn and winter is more stable than in the spring and summer. Therefore, the stable condition leads to the accumulation of the air pollutants initiated by anthropogenic sources. This, in turn, may increase metal concentration in dust deposition. In addition, in the winter, the nearby power plant changed the fuel from gas to the gas oil. This might increase the enrichments of some metals in the dust. Figure 5 shows the enrichment heat plot of Ag, B, Co, Cr, Cu, Ni, Pb, Sn, St, U, and Zn (i.e., elements belonged to groups from medium to

Fig. 4 PCA loading 3-D plot (a) and hierarchical dendrogram obtained by War's hierarchical clustering method (b), for 25 elements in dust deposition



high enrichments) in four seasons. As acquired from Fig. 5, the darker colors show the more enrichment and vice versa. For example, in the case of Pb, the order of decreasing enrichment amount is winter > autumn > summer > spring.

In a study conducted to evaluate the heavy metals contamination of dust deposition in Kurdistan province (Iran), Khuzestani and Sourı reported that heavy metals enrichment in dust deposition changes with meteorological variations (Khuzestani and Sourı 2013). In several studies on dustfall metals enrichment in other regions of the world, depending on the sampling area, types, and the location of the natural and industrial pollution sources, different patterns of enriched metals have been reported. For example, in Daejeon

(Korea), Jinan (China), Baoji (China), Bulgaria (Serbia), and Abu Zaabal (industrial area in Egypt), the decreasing order of the enrichment factors was Cd > Pb > Zn (Lee et al. 2013), Zn > Pb > Cu (Feng et al. 2012), Pb > Zn > Cr (Wang et al. 2014), Pb > Cd > Cu (Mijić et al. 2010), and Pb > Cd > Cu (Shakour Ali et al. 2011), respectively. In Illinois (the USA), in addition to the high amounts of cerium and sulfur enrichments, which indicate the coal resources in this area, the decreasing order of the enrichment factors was Hg > Zn > Cd (Lynam et al. 2014).

Table 6 represents the I_{geo} , I_{geo} class, and also the enrichment factor of elements for all sampling stations. According to Table 6, the maximum enrichment for Cu (EF = 4.09), Ni (EF = 5.91), Pb (EF = 22.24), Sn (EF = 207.39), U (EF = 53.44), and B (EF = 405.09) occurred in the MWWC station.

Table 5 I_{geo} value, I_{geo} class, and enrichment factors for dust elements in various seasons

Elements	Spring			Summer			Autumn			Winter			Annual mean		
	I_{geo} value	I_{geo} class	EF	I_{geo} value	I_{geo} class	EF	I_{geo} value	I_{geo} class	EF	I_{geo} value	I_{geo} class	EF	I_{geo} value	I_{geo} class	EF
Ag	4.81	5	143.21	5.44	6	212.44	5.76	6	195.69	5.47	6	186.88	5.41	6	185.46
Al	-2.35	0	1.00	-2.29	0	1.00	-1.85	0	1.00	-2.07	0	1.00	-2.13	0	1.00
B	6.40	6	430.66	6.83	6	556.46	6.13	6	252.52	5.05	6	139.41	6.33	6	352.26
Ba	-1.83	0	1.43	-1.83	0	1.37	-1.60	0	1.19	-1.77	0	1.23	-1.76	0	1.29
Ca	-0.38	0	3.93	-0.62	0	3.19	-0.66	0	2.28	-0.49	0	2.99	-0.53	0	3.02
Ce	-1.98	0	1.29	-1.95	0	1.26	-1.86	0	0.99	-1.84	0	1.17	-1.91	0	1.16
Co	0.36	1	6.55	0.35	1	6.24	0.80	1	6.29	0.54	1	6.12	0.53	1	6.29
Cr	-1.27	0	2.11	-0.55	0	3.34	0.64	1	5.60	0.84	1	7.53	0.21	1	5.04
Cu	-0.62	0	3.31	-0.72	0	2.97	0.03	1	3.68	-0.26	0	3.51	-0.36	0	3.40
Fe	-2.31	0	1.03	-2.47	0	0.88	-2.03	0	0.88	-2.22	0	0.90	-2.25	0	0.92
K	-4.58	0	0.21	-4.66	0	0.19	-4.70	0	0.14	-4.77	0	0.15	-4.68	0	0.17
Li	-0.03	0	5.01	0.16	1	5.46	0.03	1	3.68	-0.13	0	3.84	0.01	1	4.40
Mg	-2.48	0	0.92	-2.57	0	0.82	-2.19	0	0.79	-2.57	0	0.71	-2.44	0	0.80
Mn	-1.90	0	1.37	-1.92	0	1.29	-1.80	0	1.04	-1.89	0	1.13	-1.88	0	1.19
Na	-9.02	0	0.01	8.73	0	0.01	-9.01	0	0.01	-8.89	0	0.01	-8.91	0	0.01
Ni	-0.93	0	2.67	-0.35	0	3.84	0.19	1	4.10	0.45	1	5.76	-0.05	0	4.20
P	-1.87	0	1.40	-2.18	0	1.08	-2.12	0	0.83	-2.10	0	0.98	-2.06	0	1.04
Pb	1.59	2	15.30	1.21	2	11.31	2.36	3	18.51	2.54	3	24.49	2.02	3	17.77
Si	-7.96	0	0.02	-7.43	0	0.03	-8.96	0	0.01	-8.40	0	0.01	-8.08	0	0.02
Sn	3.67	4	64.78	3.96	4	75.92	5.47	6	159.27	5.52	6	192.92	4.89	5	129.26
Sr	0.03	1	5.21	0.06	1	5.08	-0.47	0	2.61	-0.40	0	3.19	-0.17	0	3.87
Ti	-2.35	0	1.00	-2.51	0	0.86	-2.43	0	0.67	-2.47	0	0.76	-2.44	0	0.81
U	3.31	4	50.44	2.93	3	37.22	3.57	4	42.92	3.49	4	47.43	3.35	4	44.42
V	-1.51	0	1.79	-1.52	0	1.70	-1.22	0	1.54	-1.46	0	1.53	-1.43	0	1.62
Zn	0.61	1	7.76	-0.10	0	4.57	0.84	1	6.46	1.07	2	8.83	0.67	1	6.93

Table 6 I_{geo} value, I_{geo} class, and enrichment factors for dust elements in various stations

Elements	RWWC			SBH			SPH			EO			MWWC		
	I_{geo} value	I_{geo} class	EF	I_{geo} value	I_{geo} class	EF	I_{geo} value	I_{geo} class	EF	I_{geo} value	I_{geo} class	EF	I_{geo} value	I_{geo} class	EF
Ag	5.60	6	215.09	5.33	6	162.41	5.64	6	246.72	4.75	5	107.51	5.57	6	217.57
Al	-2.15	0	1.00	-2.01	0	1.00	-2.30	0	1.00	-2.00	0	1.00	-2.19	0	1.00
B	6.23	6	332.39	6.22	6	300.85	6.31	6	391.43	6.41	6	340.26	6.47	6	405.09
Ba	-1.76	0	1.31	-1.80	0	1.16	-1.63	0	1.60	-1.77	0	1.17	-1.83	0	1.28
Ca	-0.58	0	2.98	-0.57	0	2.71	-0.59	0	3.28	-0.44	0	2.95	-0.49	0	3.25
Ce	-1.90	0	1.19	-1.83	0	1.13	-2.28	0	1.02	-1.77	0	1.17	-1.81	0	1.30
Co	0.61	1	6.77	0.51	1	5.73	0.46	1	6.79	0.66	1	6.32	0.38	1	5.94
Cr	-0.91	0	2.36	-0.63	0	2.61	0.61	1	7.53	0.54	1	5.83	0.61	1	6.96
Cu	-0.25	0	3.73	-0.30	0	3.27	-0.76	0	2.92	-0.41	0	3.00	-0.16	0	4.09
Fe	-2.12	0	1.02	-2.24	0	0.85	-2.34	0	0.97	-2.17	0	0.89	-2.38	0	0.88
K	-4.68	0	0.17	-4.69	0	0.16	-4.68	0	0.19	-4.49	0	0.18	-4.87	0	0.16
Li	-0.05	0	4.29	0.11	1	4.34	-0.09	0	4.63	0.10	1	4.28	-0.01	0	4.53
Mg	-2.68	0	0.69	-2.24	0	0.85	-2.62	0	0.80	-2.21	0	0.86	-2.52	0	0.80
Mn	-1.78	0	1.29	-1.93	0	1.06	-1.92	0	1.30	-1.71	0	1.22	-2.06	0	1.10
Na	-8.99	0	0.01	-8.91	0	0.01	-9.14	0	0.01	-8.82	0	0.01	-8.72	0	0.01
Ni	-0.63	0	2.87	-0.84	0	2.25	0.22	1	5.74	0.23	1	4.68	0.37	1	5.91
P	-2.14	0	1.01	-2.22	0	0.87	-1.88	0	1.34	-2.02	0	0.99	-2.08	0	1.08
Pb	2.11	3	19.11	2.05	3	16.68	1.60	2	15.01	2.00	2	15.95	2.28	3	22.24
Si	-8.18	0	0.02	-8.86	0	0.01	-8.07	0	0.02	-8.18	0	0.01	-7.45	0	0.03
Sn	3.97	4	69.53	4.12	5	70.29	4.99	5	157.50	5.16	6	142.78	5.51	6	207.39
Sr	-0.23	0	3.77	-0.25	0	3.39	-0.15	0	4.45	-0.01	0	3.95	-0.23	0	3.88
Ti	-2.42	0	0.83	-2.44	0	0.74	-2.46	0	0.90	-2.27	0	0.83	-2.61	0	0.75
U	3.37	4	45.78	3.23	4	37.75	3.18	4	44.83	3.38	4	41.61	3.55	4	53.44
V	-1.48	0	1.59	-1.51	0	1.42	-1.47	0	1.79	-1.24	0	1.69	-1.48	0	1.64
Zn	0.94	1	8.54	0.49	1	5.65	0.54	1	7.20	0.72	1	6.59	0.59	1	6.85

	Ag	B	Co	Cr	Cu	Ni	Pb	Sn	Sr	U	Zn	
Season	Spring	143.21	430.66	6.55	2.11	3.31	2.67	15.30	64.78	5.21	50.44	7.76
	Summer	212.44	556.46	6.24	3.34	2.97	3.84	11.31	75.92	5.08	37.22	4.57
	Autumn	195.69	252.52	6.29	5.60	3.68	4.10	18.51	159.27	2.61	42.92	6.46
	Winter	186.88	139.41	6.12	7.53	3.51	5.76	24.49	192.92	3.19	47.43	8.83
Station	RWWC	215.09	332.39	6.77	2.36	3.73	2.87	19.11	69.53	3.77	45.78	8.54
	SBH	162.41	300.85	5.73	2.61	3.27	2.25	16.68	70.29	3.39	37.75	5.65
	SPH	246.72	391.43	6.79	7.53	2.92	5.74	15.01	157.50	4.45	44.83	7.20
	EO	107.51	340.26	6.32	5.83	3.00	4.68	15.95	142.78	3.95	41.61	6.59
	MWWC	217.57	405.09	5.94	6.96	4.09	5.91	22.24	207.39	3.88	53.44	6.85

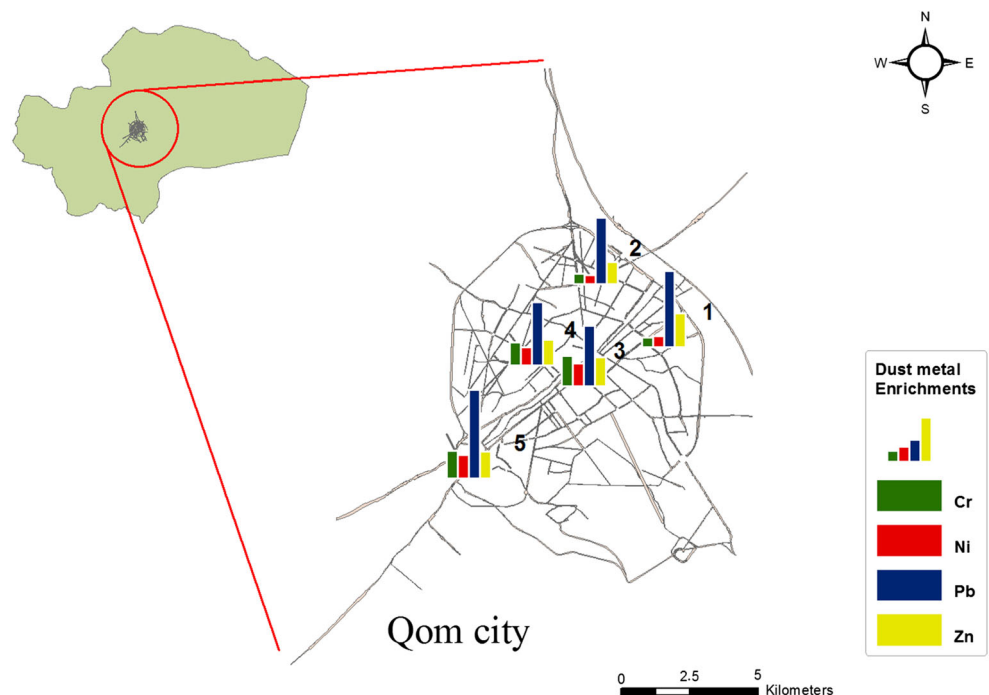
Fig. 5 Enrichment heat plot of various elements in dust deposition according to different seasons and stations

Additionally, regarding Ag (EF = 246.72), Cr (EF = 7.53), Co (EF = 6.79), and Sr (EF = 4.45), the maximum amounts occurred in the SPH station. Consequently, the maximum enrichment amounts (considerably for heavy metals) were observed in the MWWC and SPH stations. Similarly, the minimum amounts of enrichment were recorded in the SBH station.

The presence of pollutant industries, especially a power plant (at a distance of the 5 km from the southwest of city and around 8 km from MWWC sampling point), and the prevailing wind in the area (for the

MWWC station), as well as the high rate of traffic jam in the central parts of the city (for SPH station), can be considered as the causes of these alterations. Figure 5 also reveals the changes of enriched elements in different stations through heat plot. As shown in Fig. 5, seasons with more enrichment display darker colors. Figure 6 (also in graphic abstract) shows the enrichment changes of heavy metals (as histogram) consisting of chrome, nickel, lead, and zinc obtained from all sampling stations (selected metals are classified based on their importance in the environmental and health aspects).

Fig. 6 Dust metals enrichments for different stations in Qom



Conclusions

In this study, the changes of metal contents in dust deposition in Qom urban areas during different seasons were investigated. Five stations in different geographical zones of the city were selected for annual sampling.

Large concentrations were found for some elements such as Ca, Al, and Fe while trace concentrations were found for Ag, Ce, and Li (mg/kg) in dust deposition. This shows the effects of natural and desert resources in the region. There were no statistically significant differences among the concentrations of elements in different stations. However, the difference between concentrations of elements was significant in various seasons. The concentrations of elements such as Al, Cr, Pb, Sn, U, and Zn significantly increased in cold seasons. Furthermore, there was a considerable increase in the concentrations of Ni, Cu, and Co in cold seasons. These increases could be attributed to the external industrial sources, the urban traffic jam, and the effects of stable atmospheric condition in the study period. The PCA and CA showed that four components and seven clusters can be considered as the deposited elements. Thus, adjacent desert region, soil re-suspension, and anthropogenic/industrial sources can be recognized as the source of these elements. The elemental enrichment analysis of dust deposition showed that the elemental enrichment amounts decreased in the following order:

$B > Ag > U > Zn > Co > Cr > Li > Ni > Sr > Co$

These enrichment amounts demonstrate the effects of industrial sources including the combined cycle power plant in the southwest region, numerous publishing industries in the downtown, and pesticide manufacturers located around the city. Similarly, the stable weather condition of the atmosphere in the cold seasons can enhance the impact of traffic and industrial sources on metals enrichments.

Acknowledgments We would like to thank the Medical Geology Department of Geological Survey of Iran for their collaboration. The authors also wish to express their deepest gratitude to Mr. M. Zohrab Baigy for his collaboration in editing an earlier draft of this article.

Funding information This study received financial and technical supports from the Institute for Environmental Research (IER) of Tehran University of Medical Sciences (grant number 92-01-46-20879) and Research Center for Environmental Pollutants, Qom University of Medical Sciences (grant number 91334).

References

ASTM (2004) Standard test method for collection and measurement of dustfall (settleable particulate matter)

- Azarakhshi M, Mahdavi M, Arzani H, Ahmadi H (2012) Assessment of the Palmer drought severity index in arid and semi arid rangeland: (case study: Qom province, Iran). *Desert* 16:77–86
- Bellis DJ, Satake K, Inagaki M, Zeng J, Oizumi T (2005) Seasonal and long-term change in lead deposition in central Japan: evidence for atmospheric transport from continental Asia. *Sci Total Environ* 341: 149–158
- Boonyatumanond R, Murakami M, Wattayakorn G, Togo A, Takada H (2007) Sources of polycyclic aromatic hydrocarbons (PAHs) in street dust in a tropical Asian mega-city, Bangkok, Thailand. *Sci Total Environ* 384:420–432
- Brunekreef B, Holgate ST (2002) Air pollution and health. *Lancet* 360: 1233–1242
- Butean C, Berinde ZM, Mihali C, Michnea AM, Gavra A, Simionescu M (2014) Atmospheric deposition of copper and zinc in Maramures County (Romania). *Acta Chemica Iasi* 22:165–176
- Chen H, Lu X, Chang Y, Xue W (2014) Heavy metal contamination in dust from kindergartens and elementary schools in Xi'an, China. *Environ Earth Sci* 71:2701–2709
- Cheng M-F, Ho S-C, Chiu H-F, Wu T-N, Chen P-S, Yang C-Y (2008) Consequences of exposure to Asian dust storm events on daily pneumonia hospital admissions in Taipei, Taiwan. *J Toxic Environ Health A* 71:1295–1299
- Choi H, Zhang Y, Kim K (2008) Sudden high concentration of TSP affected by atmospheric boundary layer in Seoul metropolitan area during duststorm period. *Environ Int* 34:635–647
- Chung Y-s, Kim H-s, Dulam J, Harris J (2003) On heavy dustfall observed with explosive sandstorms in Chongwon-Chongju, Korea in 2002. *Atmos Environ* 37:3425–3433
- Çöl M, Çöl C (2003) Environmental boron contamination in waters of Hisarcik area in the Kutahya Province of Turkey. *Food Chem Toxicol* 41:1417–1420
- De Longueville F, Hountondji Y-C, Henry S, Ozer P (2010) What do we know about effects of desert dust on air quality and human health in West Africa compared to other regions? *Sci Total Environ* 409:1–8
- Dockery D, Pope A (1996) Epidemiology of acute health effects: summary of time-series studies. Harvard University Press, Cambridge, pp 123–147
- Feng S, Liu H, Zhang N, Lin H, Du X, Liu Y (2012) Contamination assessment of copper, lead, zinc and chromium in dust fall of Jinan, NE China. *Environ Earth Sci* 66:1881–1886
- Fouladi Fard R, Naddafi K, Yunesian M, Nabizadeh Nodehi R, Dehghani MH, Hassanvand MS (2016) The assessment of health impacts and external costs of natural gas-fired power plant of Qom. *Environ Sci Pollut Res*:1–15
- Ghrefat HA, Abu-Rukah Y, Rosen MA (2011) Application of geoaccumulation index and enrichment factor for assessing metal contamination in the sediments of Kafra Dam, Jordan. *Environ Monit Assess* 178:95–109
- Gunawardana C, Goonetilleke A, Egodawatta P, Dawes L, Kokot S (2012) Source characterisation of road dust based on chemical and mineralogical composition. *Chemosphere* 87:163–170
- Haldar P, Pavord ID, Shaw DE, Berry MA, Thomas M, Brightling CE, Wardlaw AJ, Green RH (2008) Cluster analysis and clinical asthma phenotypes. *Am J Respir Crit Care Med* 178:218–224
- Hamaiedh H, El-Hasan T (2011) Inorganic chemistry, granulometry and mineralogical characteristics of the dust fall over phosphate mine adjacent area, central Jordan. *Environ Earth Sci* 62:1771–1777
- Han Y, Cao J, Posmentier ES, Fung K, Tian H, An Z (2008) Particulate-associated potentially harmful elements in urban road dusts in Xi'an, China. *Appl Geochem* 23:835–845
- Harrad S, Ibarra C, Robson M, Melymuk L, Zhang X, Diamond M, Douwes J (2009) Polychlorinated biphenyls in domestic dust from Canada, New Zealand, United Kingdom and United States: implications for human exposure. *Chemosphere* 76:232–238

- Hsu SC, Liu SC, Huang YT, Lung SCC, Tsai F, Tu JY, Kao SJ (2008) A criterion for identifying Asian dust events based on Al concentration data collected from northern Taiwan between 2002 and early 2007. *J Geophys Res Atmos* 1984–2012:113
- IRIMO-Qom (2013) Iranian Meteorological Office Data Processing Center. Islamic Republic of Iran Meteorological Office, Qom
- Isalou AA, Litman T, Shahmoradi B (2014) Testing the housing and transportation affordability index in a developing world context: a sustainability comparison of central and suburban districts in Qom, Iran. *Transp Policy* 33:33–39
- Joshi UM, Vijayaraghavan K, Balasubramanian R (2009) Elemental composition of urban street dusts and their dissolution characteristics in various aqueous media. *Chemosphere* 77:526–533
- Kara M, Dumanoglu Y, Altioek H, Elbir T, Odabasi M, Bayram A (2014) Seasonal and spatial variations of atmospheric trace elemental deposition in the Aliaga industrial region, Turkey. *Atmos Res* 149: 204–216
- Khadivi-Khub A, Kameli M, Moshfeghi N, Ebrahimi A (2015) Phenotypic characterization and relatedness among some Iranian pomegranate (*Punica granatum L.*) accessions. *Trees* 29:893–901
- Khazaei M, Mahvi AH, Fard RF, Izanloo H, Yavari Z, Tashayoei HR (2013) Dental caries prevalence among schoolchildren in urban and rural areas of Qom province, central part of Iran. *Middle-East J Sci Res* 18:584–591
- Khuzestani RB, Soury B (2013) Evaluation of heavy metal contamination hazards in nuisance dust particles, in Kurdistan Province, western Iran. *J Environ Sci* 25:1346–1354
- Kurt-Karakus PB (2012) Determination of heavy metals in indoor dust from Istanbul, Turkey: estimation of the health risk. *Environ Int* 50: 47–55
- Kvietkus K, Šakalys J, Valiulis D (2011) Trends of atmospheric heavy metal deposition in Lithuania. *Lith J Phys* 51:359–369
- Lee P-K, Youm S-J, Jo HY (2013) Heavy metal concentrations and contamination levels from Asian dust and identification of sources: a case-study. *Chemosphere* 91:1018–1025
- Lu X, Li LY, Wang L, Lei K, Huang J, Zhai Y (2009) Contamination assessment of mercury and arsenic in roadway dust from Baoji, China. *Atmos Environ* 43:2489–2496
- Lue Y, Liu L, Hu X, Wang L, Guo L, Gao S, Zhang X, Tang Y, Qu Z, Cao H (2010) Characteristics and provenance of dustfall during an unusual floating dust event. *Atmos Environ* 44:3477–3484
- Lynam MM, Dvonch JT, Hall NL, Morishita M, Barres JA (2014) Trace elements and major ions in atmospheric wet and dry deposition across central Illinois, USA. *Air Qual Atmos Health* 8:135–147
- Marrugo-Negrete JL, Urango-Cardenas ID, Núñez SMB, Díez S (2014) Atmospheric deposition of heavy metals in the mining area of the San Jorge river basin, Colombia. *Air Qual Atmos Health* 7:577–588
- Melaku S, Morris V, Raghavan D, Hosten C (2008) Seasonal variation of heavy metals in ambient air and precipitation at a single site in Washington, DC. *Environ Pollut* 155:88–98
- Mijić Z, Stojić A, Perišić M, Rajšić S, Tasić M, Radenković M, Joksić J (2010) Seasonal variability and source apportionment of metals in the atmospheric deposition in Belgrade. *Atmos Environ* 44: 3630–3637
- Moja S, Mnisi J (2013) Seasonal variations in airborne heavy metals in Vanderbijl park, South Africa. *J Environ Chem Ecotoxicol* 5: 227–233
- Momani KA, Jiries AG, Jaradat QM (2000) Atmospheric deposition of Pb, Zn, Cu, and Cd in Amman, Jordan. *Turk J Chem* 24:231–238
- Müller G (1969) Index of geoaccumulation in sediments of the Rhine River. *GeoJournal* 2:108–118
- Mun'im Mohd Han N, Latif MT, Othman M, Dominick D, Mohamad N, Juahir H, Tahir NM (2014) Composition of selected heavy metals in road dust from Kuala Lumpur city centre. *Environ Earth Sci* 72: 849–859
- Nriagu JO (1988) A silent epidemic of environmental metal poisoning? *Environ Pollut* 50:139–161
- Pandey SK, Tripathi B, Mishra VK (2008) Dust deposition in a subtropical opencast coalmine area, India. *J Environ Manag* 86: 132–138
- Parks JL, Edwards M (2005) Boron in the environment. *Crit Rev Environ Sci Technol* 35:81–114
- Purcell TW, Peters JJ (1998) Sources of silver in the environment. *Environ Toxicol Chem* 17:539–546
- Qiao Q, Huang B, Zhang C, Piper JD, Pan Y, Sun Y (2013) Assessment of heavy metal contamination of dustfall in northern China from integrated chemical and magnetic investigation. *Atmos Environ* 74:182–193
- Rashki A, Eriksson PG, Rautenbach CW, Kaskaoutis DG, Grote W, Dykstra J (2013) Assessment of chemical and mineralogical characteristics of airborne dust in the Sistan region, Iran. *Chemosphere* 90: 227–236
- Rout T, Masto RE, Padhy P, Ram L, George J, Joshi G (2015) Heavy metals in dusts from commercial and residential areas of Jharia coal mining town. *Environ Earth Sci* 73:347–359
- Shakour Ali AA, El Taieb NM, Ibrahim AMAYH, El SGA (2011) Heavy metals enrichment in deposited particulate matter at Abu Zaabal industrial area—Egypt. *J Am Sci* 7:347–352
- Sharma RK, Agrawal M (2005) Biological effects of heavy metals: an overview. *J Environ Biol* 26:301–313
- Shin E-C, Craft BD, Pegg RB, Phillips RD, Eitenmiller RR (2010) Chemometric approach to fatty acid profiles in Runner-type peanut cultivars by principal component analysis (PCA). *Food Chem* 119: 1262–1270
- Sipos P, Kovács VK, Márton E, Németh T, May Z, Szalai Z (2012) Lead and zinc in the suspended particulate matter and settled dust in Budapest, Hungary. *Eur Chem Bull* 1:449–454
- Soriano A, Pallarés S, Pardo F, Vicente A, Sanfeliu T, Bech J (2012) Deposition of heavy metals from particulate settleable matter in soils of an industrialised area. *J Geochem Explor* 113:36–44
- Taylor SR (1964) Abundance of chemical elements in the continental crust: a new table. *Geochim Cosmochim Acta* 28(8):1273–1285
- Thakur M, Deb MK, Imai S, Suzuki Y, Ueki K, Hasegawa A (2004) Load of heavy metals in the airborne dust particulates of an urban city of central India. *Environ Monit Assess* 95:257–268
- Wang L, Lu X, Ren C, Li X, Chen C (2014) Contamination assessment and health risk of heavy metals in dust from Changqing industrial park of Baoji, NW China. *Environ Earth Sci* 71:2095–2104
- Wei B, Yang L (2010) A review of heavy metal contaminations in urban soils, urban road dusts and agricultural soils from China. *Microchem J* 94:99–107
- Wong C, Li X, Zhang G, Qi S, Peng X (2003) Atmospheric deposition of heavy metals in the Pearl River Delta, China. *Atmos Environ* 37: 767–776
- Woods WG (1994) An introduction to boron: history, sources, uses, and chemistry. *Environ Health Perspect* 102:5–11
- Yazbeck C, Kloppmann W, Cottier R, Sahuquillo J, Debotte G, Huel G (2005) Health impact evaluation of boron in drinking water: a geographical risk assessment in Northern France. *Environ Geochem Health* 27:419–427
- Yongming H, Peixuan D, Junji C, Posmentier ES (2006) Multivariate analysis of heavy metal contamination in urban dusts of Xi'an, Central China. *Sci Total Environ* 355:176–186
- Zheng N, Liu J, Wang Q, Liang Z (2010) Heavy metals exposure of children from stairway and sidewalk dust in the smelting district, northeast of China. *Atmos Environ* 44:3239–3245